Food Chemistry 473 (2025) 142962

Contents lists available at ScienceDirect

Food Chemistry

journal homepage: www.elsevier.com/locate/foodchem

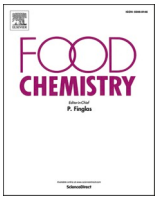

Changes of digestive stability and potential allergenicity of high hydrostatic pressure-treated ovalbumin during *in vitro* digestion

Jing Yang [a,*], Nandan Kumar [b], Hong Kuang [a], Jiajia Song [c], Yonghui Li [b,*]

[a] School of Food Science and Engineering, Chongqing Technology and Business University, Chongqing 400067, China
[b] Department of Grain Science and Industry, Kansas State University, Manhattan, KS 66506, USA
[c] College of Food Science, Southwest University, Chongqing 400715, China

ARTICLE INFO

Keywords:
Food processing
Egg white allergen
Digestion
IgE binding capacity
Molecular dynamics simulation

ABSTRACT

Food allergens are defined by their stability during digestion, with allergenicity largely influenced by resistance to enzymatic hydrolysis. Ovalbumin (OVA), a major egg protein, is a significant contributor to food allergies, particularly in children. Our previous work demonstrated that high hydrostatic pressure (HHP) treatment reduces OVA allergenicity by disrupting conformational epitopes and altering its structure. This study hypothesizes that HHP further influences OVA digestibility, allergenicity, and molecular structure during digestion. Results show that HHP treatment (600 MPa) reduced α-helix content by 16.1 % and increased β-sheet content by 38.4 %, enhancing free sulfhydryl groups and surface hydrophobicity. Hydrolysis and ELISA analyses confirmed that HHP accelerated enzymatic hydrolysis, significantly reducing OVA allergenicity. Molecular dynamics simulations revealed strengthened interactions between OVA and pepsin/trypsin, involving epitope residues. These findings indicate an association between HHP treatment and the modification of OVA's digestive stability and epitopes, suggesting its potential as a strategy for reducing allergenicity.

1. Introduction

Egg white is a widely utilized food ingredient and an important source of high-quality dietary protein, renowned for its exceptional digestibility, balanced amino acid composition, functional properties (including gelling, foaming, and emulsification), and desirable sensory attributes. However, it is also a common allergen, affecting 1.6 % to 10.1 % of individuals worldwide, thereby representing a significant public health concern (Taniguchi, Ogura, Sato, Ebisawa, & Yanagida, 2022; Zhu, Vanga, Wang, & Raghavan, 2018).

One of the key characteristics of food allergens is their stability during digestion. The allergenicity of proteins is influenced by their resistance to enzymatic hydrolysis in the gastrointestinal tract (Pekar, Ret, & Untersmayr, 2018). The ability of allergenic proteins to remain intact and cross the gastrointestinal mucosa is crucial, as the retention of linear and conformational epitopes allows these proteins to bind to IgE antibodies, potentially triggering severe allergic reactions (Bu, Luo, Chen, Liu, & Zhu, 2013). *In vitro* digestion, a method simulating gastric and intestinal processes, is commonly employed to study food protein digestibility due to its simplicity, efficiency, low cost, and reproducibility (Brodkorb et al., 2019). Ovalbumin (OVA), which accounts for 54 % of egg white protein by weight, is a major egg white allergen (Horvitz, Arroqui, & Vírseda, 2024). OVA exhibits high resistance to pepsin hydrolysis, retaining its immunoreactivity against IgE from allergic patients' sera after gastric digestion, though this reactivity diminishes considerably after duodenal digestion (Martos, Contreras, Molina, & Lopez-Fandino, 2010). Despite enzymatic hydrolysis and *in vitro* digestion, the IgE-binding capacities of egg white proteins are not completely eliminated (Behzad Gazme, Rezaei, & Udenigwe, 2020). Thus, applying advanced processing techniques to OVA could enhance its digestibility in the gastrointestinal tract while reducing its allergenicity.

Reducing protein allergenicity through food processing techniques has become a focus of research aimed at mitigating food allergies. Non-thermal processing techniques, such as high hydrostatic pressure (HHP), have garnered attention due to their ability to preserve food's nutritional components, color, and freshness (Hogan, Kelly, & Sun, 2005). HHP applies pressures up to 1000 MPa in a liquid medium within a closed system, disrupting non-covalent bonds (*e.g.*, hydrogen bonds, hydrophobic and ionic interactions) without significantly affecting covalent bonds (Boukil, Marciniak, Mezdour, Pouliot, & Doyen, 2022). By altering protein structures (secondary, tertiary, and quaternary), HHP induces new interactions and modifies physicochemical properties,

* Corresponding authors.
E-mail addresses: jyang@ctbu.edu.cn (J. Yang), yonghui@ksu.edu (Y. Li).

https://doi.org/10.1016/j.foodchem.2025.142962
Received 2 October 2024; Received in revised form 13 January 2025; Accepted 16 January 2025
Available online 23 January 2025

offering potential for reducing protein allergenicity (Bavaro et al., 2018; Wang et al., 2021a; Zhang et al., 2018). Studies using *in vitro* digestion have demonstrated that non-thermal techniques (*e.g.*, ultrasound, HHP, and irradiation) not only modify food protein conformations but also enhance digestibility, potentially reducing allergenicity (Chicón, Belloque, Alonso, & López-Fandiño, 2008; Wang et al., 2021; Wang, Wang, Vanga, & Raghavan, 2021). HHP treatment has been shown to reduce the allergenicity of milk proteins (Chicón et al., 2008; Zeece, Huppertz, & Kelly, 2008), and combined thermal/pressure processing diminishes allergenic properties in shrimp (Liu et al., 2023), peanuts (Bavaro et al., 2018), and almonds (De Angelis, Bavaro, Forte, Pilolli, & Monaci, 2018) during gastrointestinal digestion. Our recent findings revealed that HHP alters the structure and allergenicity of OVA (Yang, Kuang, Kumar, Song, & Li, 2024). Specifically, HHP reduces OVA allergenicity by disrupting conformational epitopes and altering its structures, such as reducing α-helix content and unfolding tertiary structures (Yang et al., 2024). However, the impact of HHP on OVA's enzymatic hydrolysis and allergenicity during gastrointestinal digestion remains unclear.

We hypothesize that HHP treatment improves the digestibility of OVA in the gastrointestinal tract while reducing its allergenicity by altering its structural and physicochemical properties. In this study, we conducted *in vitro* simulated gastrointestinal digestion to investigate the structural, physicochemical, and allergenicity changes of OVA following HHP treatment. Techniques including SDS-PAGE, degree of hydrolysis analysis, circular dichroism, and fluorescence spectroscopy were utilized. Additionally, molecular dynamics (MD) simulations and ELISA were employed to evaluate changes in conformational epitopes and allergenicity during digestion.

2. Materials and methods

2.1. Reagents and materials

OVA (A5503) and 1-anilinonaphthalene-8-sulfonate (ANS, A1028) were purchased from Sigma-Aldrich (St. Louis, MO, USA). Antibodies (SA5–10262, SA5–10263) were sourced from Thermo Fisher (Shanghai, China), while pepsin (P8160, 250 units/mg) and trypsin (T8150, 250 units/mg) were obtained from Solarbio (Beijing, China). Reagents for SDS-PAGE and other analyses were from Beyotime Biotechnology (Shanghai, China), and all chemicals were of analytical grade.

2.2. HHP treatments

OVA solution (1 mg/mL) was prepared with distilled water, sealed in polyethylene bags (BZD085, Blueberry, Shanghai, China), and treated with HHP (SHPP-2 L, Shanxi, China) at 0.1 MPa, 300 MPa, 400 MPa, 500 MPa, and 600 MPa for 10 min at 25 °C. The samples were then immediately frozen at −80 °C and freeze-dried for further analysis.

2.3. In vitro digestion

In vitro digestion was carried out using both pepsin and trypsin added to the simulated gastric fluid (SGF) and simulated intestinal fluid (SIF) according to previous studies (Brodkorb et al., 2019; Jiang, Xia, Zhang, Chen, & Liu, 2020; X. Wang et al., 2022), with some modifications. To simulate gastric digestion, SGF (1.25×) was preheated in an incubator at 37 °C. OVA in simulated salivary fluid (100 mg/mL) was mixed with SGF at a 1:1 ratio, and adjusted the pH to 3.0 ± 0.1 using 1 mol/L HCl. 0.3 mol/L $CaCl_2$ was added to achieve a final concentration of 0.075 mmol/L in the digestion mixture. Porcine pepsin solution was prepared with 1.25× SGF electrolyte stock solution, and added to the digestion mixture (final concentration of 600 U/mL). The mixture was kept at 200 rpm and 37 °C for 2 h. The gastric digestion was terminated by adjusting the pH to 7.0 ± 0.1 using 1 mol/L NaOH.

For simulated intestinal digestion, SIF (1.25×) was preheated in a water bath at 37 °C. The gastric digestion liquid was mixed with SIF in a 1:1 ratio and adjusted the pH to 7.0 ± 0.1 using 1 mol/L NaOH. Porcine bile salt was added to reach a final concentration of 10 mmol/L, then the solution was incubated at 200 rpm and 37 °C for 40 min to ensure complete dissolution of the bile. 0.3 mol/L $CaCl_2$ was added to achieve a final concentration of 0.3 mmol/L in the digestion mixture. Trypsin solution was prepared and added to the mixture for a final concentration of 100 U/mL. The mixture was kept at 200 rpm and 37 °C for 2 h. After the intestinal digestion, treat the mixture at 95 °C for 5 min, then freeze-dry the sample.

2.4. Analysis of IgE-binding ability

The IgE-binding capacity of OVA was analyzed according to our method (Yang et al., 2024). First, untreated or HHP-treated OVA was dissolved in carbonate buffer (50 mmol/L, pH 9.6). The prepared OVA solution (100 μL/well) was added to a 96-well ELISA plate and incubated overnight at 4 °C. After incubation, the plate was emptied, and the wells were washed three times with phosphate-buffered saline containing 0.05 % Tween 20 (PBST), then gently tapped dry. Blocking buffer (5 % skimmed milk in PBST) was added, and the plate was incubated at 37 °C for 1 h. Following this, the blocking buffer was discarded, the wells were washed three times with PBST, and 50 μL of OVA-allergic mouse serum (diluted 1:100 in PBST, prepared in our previous study (Yang et al., 2024) was added and incubated at 37 °C for 1 h. After incubation, the solution was discarded, the wells were washed five times with PBST, and IgE-HRP (diluted 1:2000 in PBST) was added and incubated at 37 °C for 30 min. The wells were then washed five times with PBST, followed by the addition of 100 μL of TMB to each well and incubation at 37 °C for 15 min. Finally, 50 μL of stop solution (2 mol/L sulfuric acid) was added, and absorbance at 450 nm was measured using a microplate reader (Infinite M200 Pro, Tecan, Männedorf, Switzerland).

2.5. Sodium dodecyl sulfate-polyacrylamide gel electrophoresis (SDS-PAGE)

OVA molecular weight changes were analyzed as described in our previous method (Yang et al., 2024). OVA solution (1 mg/mL) was mixed with 2× SDS-PAGE loading buffer at a 1:1 ratio and heated in boiling water for 10 min. A 12 % separating gel and 5 % stacking gel were prepared, and samples were loaded for electrophoresis. The run was initially set at 80 V for 20 min to allow proteins to migrate through the stacking gel, followed by 110 V for 60 min to separate proteins in the resolving gel. After electrophoresis, the gel was stained using a Fast Silver Stain Kit (Beyotime, Shanghai, China). Silver staining was performed at room temperature for 10 min, followed by incubation in 100 mL stop solution for 5 min, as per the kit protocol. The gel was then rinsed twice with 100 mL deionized water to achieve clear visualization of the separated protein bands.

2.6. Scanning electron microscope (SEM) analysis

OVA samples were coated with conductive adhesive and sputter-coated with a thin layer of gold. Their microstructure was observed using a scanning electron microscope (SEM) (SU-3500, Hitachi, Tokyo, Japan) at 5 kV with magnifications of 50× and 500 × .

2.7. Determination of degree of hydrolysis

The degree of hydrolysis of OVA samples was determined following the previous method (Nielsen, Petersen, & Dambmann, 2001). The procedure is as follows: 3 mL of OPA reagent was mixed with 400 μL of each sample evenly, allowed the reaction to proceed for 2 min, and measure the absorbance at 340 nm. Serine standard solution and distilled water were used as the standard and blank controls, respectively. The DH (degree of hydrolysis) is calculated using the following

formula:

$$\text{Serine } NH_2 = \frac{(A_{sample} - A_{blank}) \times 0.9516}{(A_{standard} - A_{blank}) \times C}$$

$$DH(\%) = \frac{\text{Serine } NH_2}{\alpha \times h_{tot}} \times 100$$

where $A_{standard}$, A_{sample}, and A_{blank} were the absorbance values of the standard, sample, and blank control, respectively; C was the concentration of the sample; according to previous method, when the raw material has not been previously analyzed, the values of α and β were assumed to be 1.00 and 0.40, respectively (Nielsen et al., 2001).

2.8. Circular dichroism analysis

The secondary structure changes of ultrasound-treated OVA were evaluated using circular dichroism (CD) spectroscopy (Chirascan, Applied Photophysics, Leatherhead, UK). OVA samples (0.2 mg/mL) were scanned at 25 °C with a wavelength range of 190–240 nm, a 1.0 nm bandwidth, and a scan rate of 100 nm/min. Ellipticity was recorded in millidegrees (mdeg), and CDNN software was used to analyze the relative content of secondary structures (α-helix, β-sheet, β-turn, and random coil) (Yang et al., 2024).

2.9. Intrinsic fluorescence spectrum analysis

The sample (0.1 mg/mL) was analyzed using a fluorescence spectrometer (F-7000, Hitachi, Tokyo, Japan). Measurement conditions were set with an excitation wavelength of 280 nm, emission range of 310–400 nm, slit widths of 5 nm, a scan rate of 1200 nm/min, and a PMT voltage of 400 V (Yang et al., 2024).

2.10. Exogenous fluorescence spectrum analysis

ANS (4 mmol/L in PBS) was mixed with OVA samples (0.1 mg/mL) at a 1:50 (*v*/v) ratio. The exogenous fluorescence spectra of ultrasound-treated OVA were measured with a fluorescence spectrometer (F-4700, Hitachi, Tokyo, Japan) under the following conditions: excitation at 390 nm, scan range of 440–600 nm, slit width of 10 nm, PMT voltage at 400 V, and a scan speed of 1200 nm/min (Yang et al., 2024).

2.11. Free sulfhydryl (SH) analysis

OVA solution (1 mg/mL) was prepared using glycine buffer. Ellman's reagent was mixed with the sample solution at a 1:100 (v/v) ratio. The mixture was then incubated in the dark at 25 °C for 1 h, after which the absorbance was measured at 412 nm using a UV spectrophotometer (UV-1102, Tianmei Techcomp, Shanghai, China). The free sulfhydryl content was calculated using the following formula: SH (μmol/g) = 73.53 × A_{412}/C, where A_{412} is the absorbance at 412 nm and C is the sample concentration (Yang et al., 2024).

2.12. Surface hydrophobicity

ANS was used as a fluorescent probe to measure the surface hydrophobicity of OVA (Y. Li et al., 2022; Yang et al., 2024). OVA samples were diluted to concentrations of 0.05, 0.1, 0.15, 0.2, and 0.25 mg/mL using PBS. Subsequently, 20 μL of 8 mmol/L ANS solution was added to 4 mL of each OVA sample solution and thoroughly mixed. The mixtures were incubated in the dark at 25 °C for 15 min. Fluorescence intensity was then measured with an excitation wavelength of 390 nm and an emission wavelength of 470 nm using a fluorescence spectrophotometer (F-4700, Hitachi, Tokyo, Japan).

2.13. Zeta potential analysis

The OVA samples were dissolved in PBS at a concentration of 1 mg/mL. The sample solution was allowed to equilibrate for 120 s prior to measurement. The zeta potential was then measured using a zeta potential analyzer (ZEV3600, Malvern Instruments, Malvern, UK) (Li, Li, Tan, Liu, & Duan, 2019; Yang et al., 2024).

2.14. Computational modeling and analysis

The sequences of pepsin and trypsin from *Gallus gallus* (Chicken) were obtained from the UniProt database under accession IDs P00793 and Q90627, respectively. For pepsin, the sequence includes a propeptide region spanning positions 1–42, which is an inactive segment that must be cleaved to activate the enzyme. Similarly, trypsin has a signal peptide (positions 1–15) and a propeptide region (positions 16–25). To model the active forms of these enzymes, the propeptide and signal peptide regions of the AlphaFold structures AF-P00793-F1 and AF-Q90627-F1 were removed, resulting in mature sequences for Pepsin (positions 43–367) and Trypsin (positions 26–248). Both structures were verified to have very high pLDDT scores (>90), indicating high confidence in their predicted folds (Varadi et al., 2022). The structure of OVA protein was taken from our previous study (Yang et al., 2024). The OVA-pepsin and OVA-trypsin were first subjected to short molecular dynamics simulations to equilibrate the models. Subsequently, protein-protein docking simulations were conducted using the HDOCK server (Yan & Huang, 2020) to explore interactions of pepsin and trypsin with OVA. The resulting protein-protein complexes were subsequently subjected to extended 500 ns MD simulations to gain a comprehensive understanding of their conformational dynamics and interaction modes. PDBePISA was used to analyze the structural characteristics of the OVA-pepsin and OVA-trypsin complexes, focusing on their interaction area and respective energies at varying pressures (Krissinel & Henrick, 2007). These results provided valuable insights into how high-pressure conditions influence the stability, binding affinity, and accessibility of IgE-binding epitopes during the digestion process.

A MD simulation of the OVA-pepsin and OVA-trypsin complexes was conducted with GROMACS version 2023.3 (Abraham et al., 2015), using the CHARMM force field (Bjelkmar, Larsson, Cuendet, Hess, & Lindahl, 2010) and solvating the system in the TIP3P water model. The protein complexes were neutralized by adding the counter ions into the solvated box depending on the charge of the protein. Energy minimization was carried out through 2000 steps of steepest descent followed by 5000 steps of conjugate-gradient minimization to ensure proper relaxation (Kumar Sarma & Sastry, 2022; Kumar & Sastry, 2021). The system was equilibrated under NVT and NPT conditions for 500 ps and 1000 ps, respectively. Subsequently, a production simulation was performed for a total duration of 5 μs, with individual simulation lasting 500 ns each, using an integration time step of 0.2 ps. The LINCS algorithm was employed to constrain all bonds, and the system was maintained at 298.15 K with a V-rescale thermostat. Trajectories were recorded every 2 ps, and pressure coupling was managed using the isotropic Parrinello-Rahman method at pressures of 0.1 MPa, 300 MPa, 400 MPa, 500 MPa, and 600 MPa.

2.15. Statistical analysis

All images were created and edited using GraphPad Prism 9 (GraphPad Software, San Diego, CA, USA). The experiments and analyses were performed in triplicate, with results reported as mean ± standard deviation. Data analysis was conducted using one-way ANOVA followed by Duncan's multiple range test, with a significance level set at $p < 0.05$, in SPSS Statistics 23 (IBM, Chicago, IL, USA).

3. Results and discussion

3.1. Effects of HHP on the microstructure and enzymolysis of OVA

This study examined the effects of HHP on the microstructure of ovalbumin (OVA) using SEM at 50× and 500× magnifications. As illustrated in Fig. 1A-B, the pre-digestion microstructure of OVA displayed a smooth, regular, sheet-like appearance. Following simulated gastrointestinal digestion, OVA was hydrolyzed into irregular fragments, with the surface becoming rough and pitted. Increasing pressure further intensified the degree of fragmentation, roughness, and aggregation compared to digested native OVA at atmospheric pressure (0.1 MPa).

SDS-PAGE analysis was performed to assess the impact of digestion on the molecular weight of OVA. As shown in Fig. 1C, digestion resulted in a lighter OVA protein band and the emergence of a new band around 15 kDa. After HHP treatment, the increased density of the 15 kDa protein band suggests that HHP promoted OVA hydrolysis during digestion, producing smaller molecular weight proteins. The effect of HHP on the degree of OVA hydrolysis during *in vitro* digestion is presented in Fig. 1D. Compared to the 0.1 MPa group, the degree of hydrolysis did not significantly change with 300 MPa treatment. However, as pressure increased, the degree of hydrolysis was positively correlated with pressure, reaching 11.4 % at 600 MPa. These findings indicate that HHP treatment was associated with structural modifications of OVA, facilitating its hydrolysis by proteases during digestion.

3.2. Effects of HHP on the molecular structure of OVA

CD spectroscopy is a valuable tool for analyzing changes in protein secondary structure. The CD spectra of OVA treated with HHP are shown in Fig. 2A-B, revealing significant attenuation near 192 nm, 208 nm, and 222 nm, indicating disruption of the α-helix structure. Compared to the 0.1 MPa group, HHP-treated OVA showed a significant decrease in α-helix content and a significant increase in β-sheet content after *in vitro* simulated digestion ($p < 0.05$). In the 600 MPa group, α-helix content decreased by 16.1 %, while β-sheet content increased by 38.4 %. Additionally, endogenous fluorescence intensity of digested OVA decreased, with a red shift in the maximum absorption emission wavelength at 600 MPa (Fig. 2C). This suggests OVA unfolded during enzymatic hydrolysis, exposing side chains and creating a more polar environment around tryptophan residues. Exogenous fluorescence intensity also increased with HHP intensity, indicating structural changes in OVA. These findings indicate that HHP treatment is associated with alterations in the spatial structure of OVA during gastrointestinal digestion, including reduced α-helix content and increased structural unfolding.

3.3. Effects of HHP on the physical properties of OVA

Zeta potential is a key parameter for assessing the aggregation state of proteins, with a decrease in absolute values indicating fewer negatively charged residues on the protein surface (Jin, Okagu, Yagoub, & Udenigwe, 2021). Compared to the undigested OVA, the zeta potential of OVA was significantly reduced after *in vitro* digestion, and no significant changes in zeta potential were observed among 0.1, 300 and 400 MPa groups. However, at higher pressures, the zeta potential significantly decreased by 30 % at 500 MPa and 76.6 % at 600 MPa, compared with 0.1 MPa group (Fig. 2E). Free sulfhydryl content, correlated with disulfide bond formation, reflects the balance between -SH groups and S—S bonds. In the 0.1 MPa group, free sulfhydryl content was 7.38 μmol/g, increasing to a maximum of 59.9 μmol/g at 600 MPa (Fig. 2F). Surface hydrophobicity remained unchanged at low pressures (300–400 MPa) but increased fourfold at 600 MPa (Fig. 2G). These findings

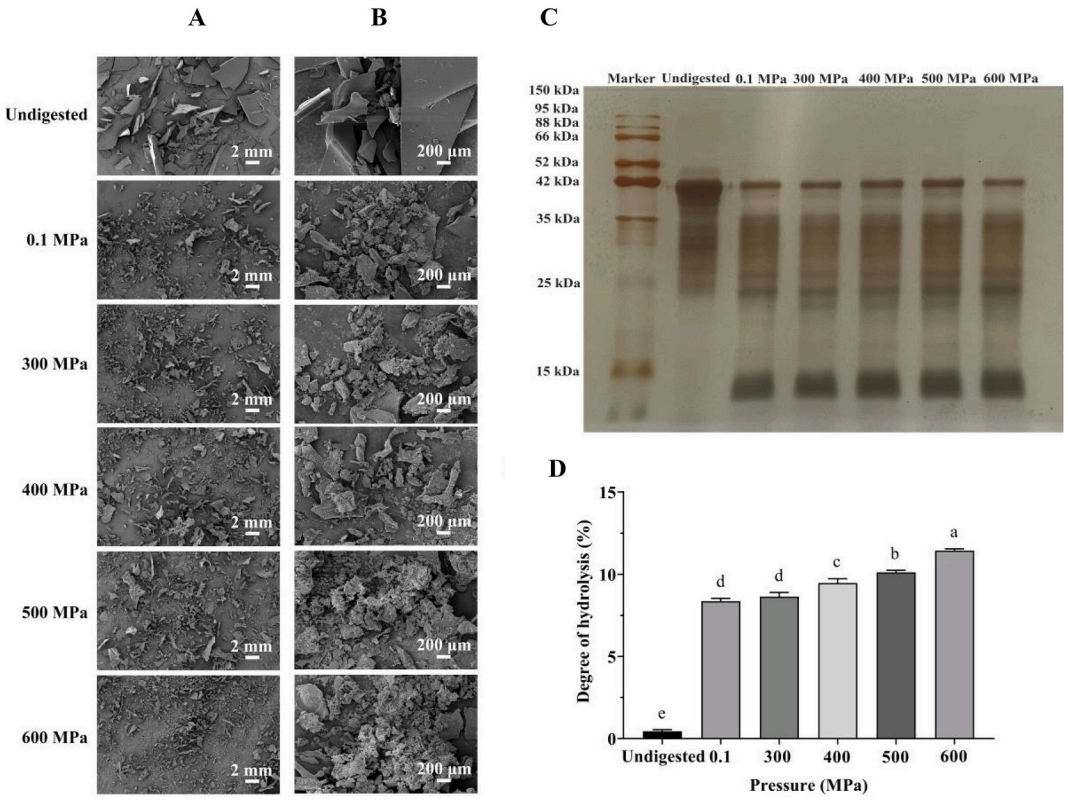

Fig. 1. The microstructure changes, molecular weight and hydrolysis of OVA treated with high hydrostatic pressure after *in vitro* digestion. SEM images of OVA at 50 × magnification (A) and 500 × magnification (B); SDS-PAGE protein bands of OVA (C); Degree of hydrolysis (D). Data are presented as the mean ± standard error of the mean (SEM), $n = 3$. Different letters in Fig. 1D indicate significant difference ($p < 0.05$).

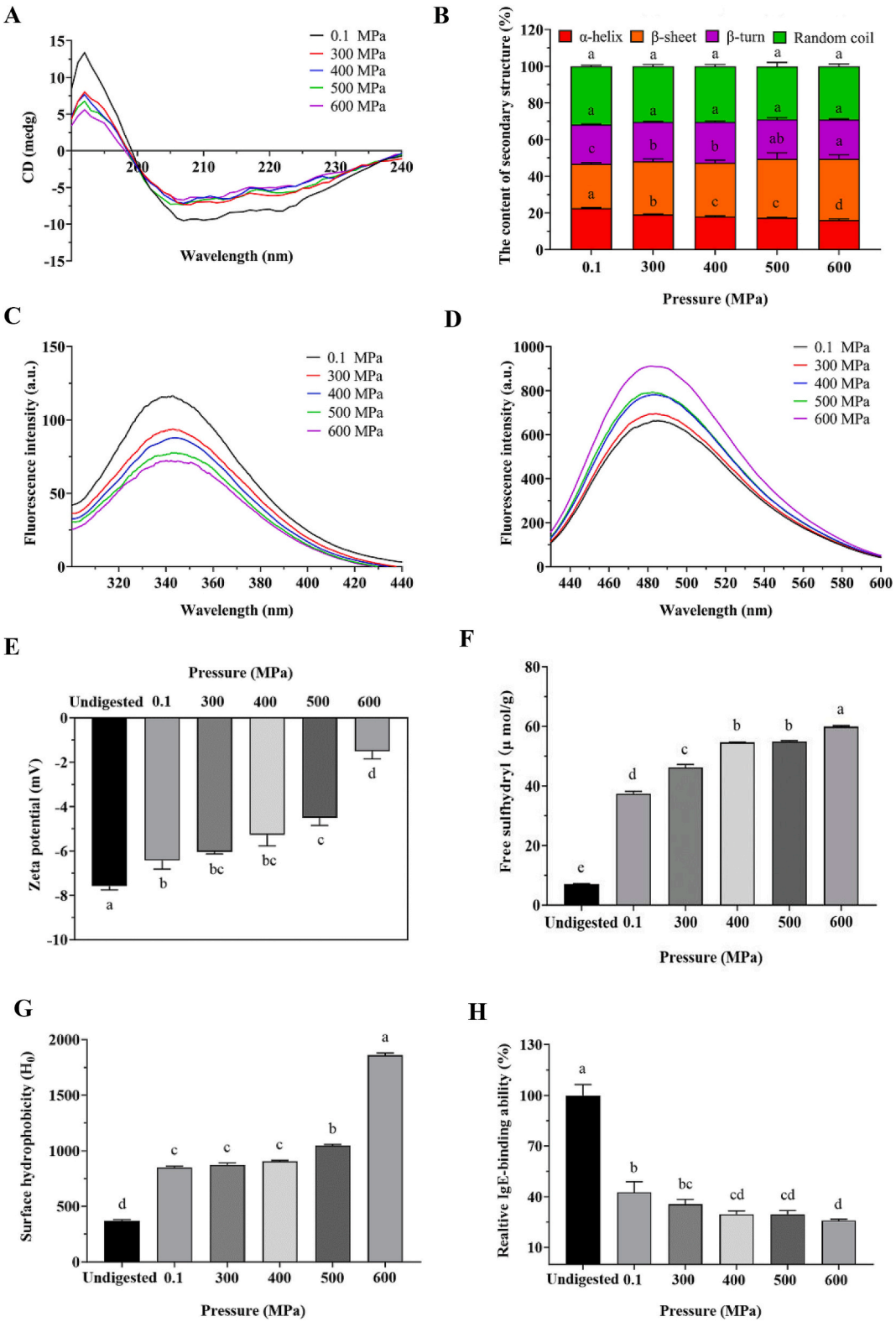

Fig. 2. The changes of molecular structure, physical properties and Ig*E*-binding capacity of OVA treated with high hydrostatic pressure after *in vitro* digestion. (A) Circular dichroism spectra; (B) Secondary structure changes of OVA; (C) Intrinsic fluorescence spectra; (D) Exogenous fluorescence spectra; (E) Zeta potential; (F) Content of free surface sulfhydryl groups; (G) Surface hydrophobicity; (H) IgE-binding capacities of OVA. Data are presented as the mean ± standard error of the mean (SEM), n = 3. Different letters in Fig. E-H indicate significant difference ($p < 0.05$).

suggest that HHP treatment is associated with the disruption of intramolecular disulfide bonds in OVA during digestion, leading to the unfolding of its tertiary structure and the exposure of hydrophobic groups.

3.4. Effect of HHP on the changes of IgE-binding capacity of OVA

Compared to undigested OVA, *in vitro* digestion with digestive enzymes reduced OVA allergenicity, with HHP treatment further enhancing this reduction (Fig. 2H). The polyclonal antibody, may provide a more extensive epitope recognition range than the monoclonal antibody, has a higher chance of binding to OVA. A similar trend was observed with monoclonal OVA-IgE antibodies (Fig. S1). Among the HHP-treated groups, the 600 MPa treatment resulted in the lowest IgE-binding ability. These findings suggest that digestive enzymes disrupt some allergenic epitopes of OVA, limiting recognition by IgE receptors. HHP treatment at 600 MPa likely enhances interactions between OVA and pepsin/trypsin, leading to more extensive epitope breakdown compared to 300 MPa.

3.5. Protein-protein docking analysis of OVA-pepsin complex and OVA-trypsin complex

Protein-protein docking was conducted to investigate the binding interactions between OVA and the digestive enzymes pepsin and trypsin under various HHP conditions (0.1 MPa to 600 MPa), as depicted in Fig. 3A-D and Fig. S2–3. The OVA structure, previously simulated in this study, was docked with the enzymes, and the top complexes were selected based on docking scores. Both pepsin and trypsin demonstrated consistent binding affinities, with docking scores of −243.55 and −239.62, respectively, and ligand RMSD values around 71 Å (Fig. S3). During the docking process, the ligand underwent conformational rearrangement to optimally fit into the protein pocket (OVA), achieving a configuration that facilitated stronger binding. Notably, the RMSD value of 71 Å was the lowest among the top ten docked complexes, indicating that this pose represents the most favorable binding configuration identified by the docking algorithm. Interaction analysis identified key residues involved in binding: at the N-terminus, His22, His23, Glu26, and Asn25 were critical; in the central region, residues such as Gln163, Pro164, Ser165, and Ser166 interacted with both enzymes, while Asp168 and Gln170 were specific to pepsin. At the C-terminus, Lys291, Thr295, and Ser296 were essential for binding with both enzymes, while additional residues, including Met299, Phe307, and Ser325, were specific to pepsin, and Val328 and Pro386 were unique to trypsin (Fig. 3D).

Regions from Met299 to Gln326 and Val328 to Pro386, which interact with both enzymes, were also identified as epitopes in the previous studies (Behzad Gazme, Rezaei, & Udenigwe, 2022; Yang et al., 2024). Fig. 2E illustrates the structural and conformational changes in OVA when bound to pepsin under varying pressures. Notable alterations in the β-sheet structure were observed at the pepsin binding sites, particularly in the Met286-Met288, Val328-Ile335, and Met173-Gly183 regions. High-pressure conditions caused an elongation of the β-sheet structure in the Met288-Met289 and Val328-Ile335 regions, while a reduction in β-sheet content was noted in the Met173-Gly183 region. These findings suggest that the overall increase in β-sheet content, as identified through CD spectroscopy (Fig. 2B), is primarily driven by changes in the Met288-Met289 and Val328-Ile335 regions. Similar β-sheet structural changes were also observed in OVA complexes with trypsin (Fig. 3F).

3.6. Effects of HHP on the conformational changes and interaction mode of OVA-pepsin and OVA-trypsin complexes

To evaluate the effects of HHP on the conformational changes and interaction mode of the complexes, we conducted detailed MD simulations of the OVA component in both the OVA-pepsin and OVA-trypsin complexes under varying pressure conditions to reveal important insights into their structural dynamics, focusing on the radius of gyration (Rg) of OVA and its corresponding free energy. For the OVA-pepsin complex, the result showed a consistent trend toward compact and stable structures as pressure increases, with relatively stable conformations across the pressure range (0.1 MPa to 600 MPa), as shown in Fig. 4. The Rg values for OVA in OVA-pepsin remain within a narrow range (2.158 Å to 2. 251 Å) where the higher pressures consistently drive OVA toward more compact structures, enhancing stability while reducing conformational variability. Free energy values also decrease smoothly, suggesting a gradual stabilization of the complex as the pressure increases. In contrast, the OVA of the OVA-trypsin complex exhibits more variability in its Rg and free energy values. At 0.1 MPa, the trypsin complex displays a larger range of Rg values, indicating greater conformational flexibility. As pressure increases, this variability reduces, but the OVA-trypsin complex still shows more pronounced changes in Rg and free energy compared to OVA-pepsin. This suggests that trypsin induces more structural fluctuations in the OVA complex at lower pressures and stabilizes only at higher pressures (600 MPa), where it achieves compactness similar to the pepsin complex (Fig. 4). These differences imply that pepsin may form a more stable and compact complex with OVA across all pressures, while trypsin exhibits more flexibility at lower pressures but eventually stabilizes at high pressure. The conformation with the lowest free energy was selected for further analysis as it likely represents the most stable complexes under the influence of HHP.

We then investigated the key residues involved in forming non-covalent interactions with digestive enzymes, as these interactions play a significant role in the stability of proteins and interactions between proteins (Krissinel & Henrick, 2007; Y. B. Kumar et al., 2024; Y. B. Kumar et al., 2023). A network of hydrogen bonds and other non-bonded interactions were identified, involving critical OVA residues such as Ser296, Lys323, and Ser325 with pepsin, and Glu18, Glu26, Glu289, and Ser296 with trypsin, which play a central role in anchoring the enzyme-substrate complex, regardless of changes in pressure, as shown in Fig. 5 and Fig. S4. Under high-pressure treatment, new hydrogen bond interactions formed between residues such as Glu26, Pro164, and Asp168 of OVA with pepsin, and Ser165, Ser166, and Asn293 of OVA with trypsin, suggesting additional stabilization of the enzyme-substrate complexes at higher pressures (Fig. 5). Moreover, multiple non-bonded interactions were observed, further contributing to the stabilization of the complexes. These interactions were reinforced by the formation of salt bridges, providing additional electrostatic stability (Fig. S4 and Table S1). This analysis offers insights into the molecular mechanisms of enzyme-substrate recognition, highlighting the significance of these residues in facilitating digestion. Notably, residues involved in hydrogen bond interactions such as Pro164, Asp168, Phe307, Ser308, Lys323, and Ser325 of OVA with pepsin, and Asn160, Gln163, Pro164, Ser165, and Ser166 of OVA with trypsin have been previously identified as epitope residues in experimental investigations and our previous study (Behzad Gazme et al., 2022; Yang et al., 2024). Additionally, other residues involved in non-bonded interactions were also identified as epitope residues, as depicted in Fig. 5 and Fig. S4. These findings suggest that the involvement of epitope residues in enzyme interactions may affect IgE-binding epitopes within the protein, potentially reducing the allergenicity of OVA.

The impact of pressure on interaction dynamics is summarized in Table 1. At 0.1 MPa, the OVA-pepsin complex exhibits a total surface area of 30,764.5 $Å^2$ and an interaction free energy (ΔGint) of −0.9 kcal/mol, indicating a relatively weak interaction. As pressure increases to 300 MPa, the surface area slightly decreases to 29,839.8 $Å^2$, while ΔGint becomes more negative at −1.5 kcal/mol, suggesting stronger binding. This trend continues at 400 MPa and 500 MPa, with ΔGint values of −0.8 and − 4.2 kcal/mol, respectively. At 600 MPa, ΔGint reaches −6.1 kcal/mol, representing the strongest interaction observed, with notable

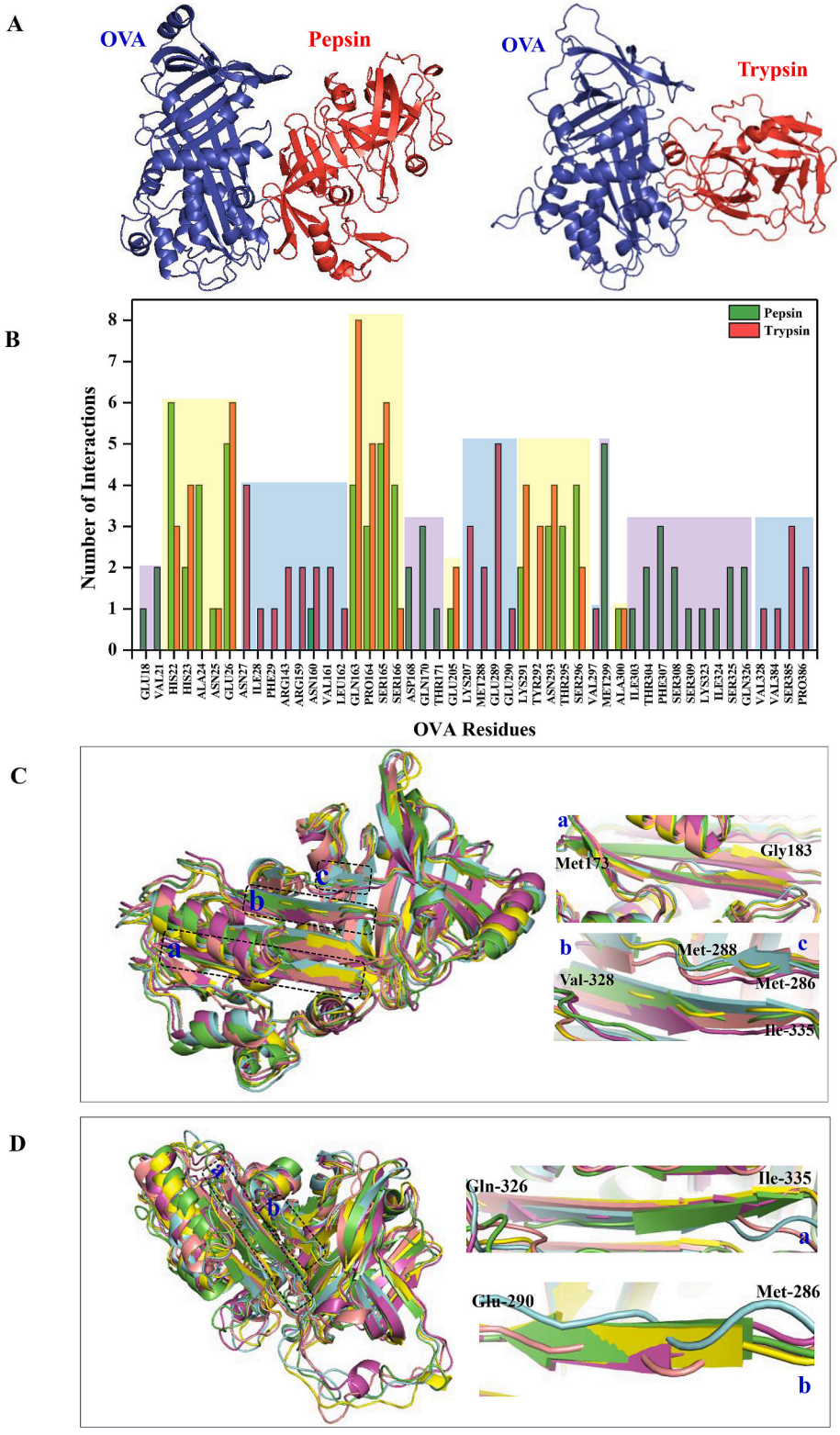

Fig. 3. Conformational changes in high hydrostatic pressure-treated OVA during *in vitro* digestion based on molecular dynamics simulations. (A) Docked complexes of OVA with pepsin or trypsin; (B) Comparative analysis of OVA residue interactions with pepsin and trypsin, highlighting the frequency of interactions, with yellow-shaded bars representing residues common to both pepsin and trypsin interactions, purple-shaded bars for residues specific to pepsin, and blue-shaded bars for residues specific to trypsin. Structural changes in the β-sheet and other regions at the pepsin-binding site and zoomed-in views of these regions in OVA-pepsin complex (C) and OVA-trypsin complex (D), obtained at 0.1 MPa (green), 300 MPa (light blue), 400 MPa (magenta), 500 MPa (yellow), and 600 MPa (orange). (For interpretation of the references to color in this figure legend, the reader is referred to the web version of this article.)

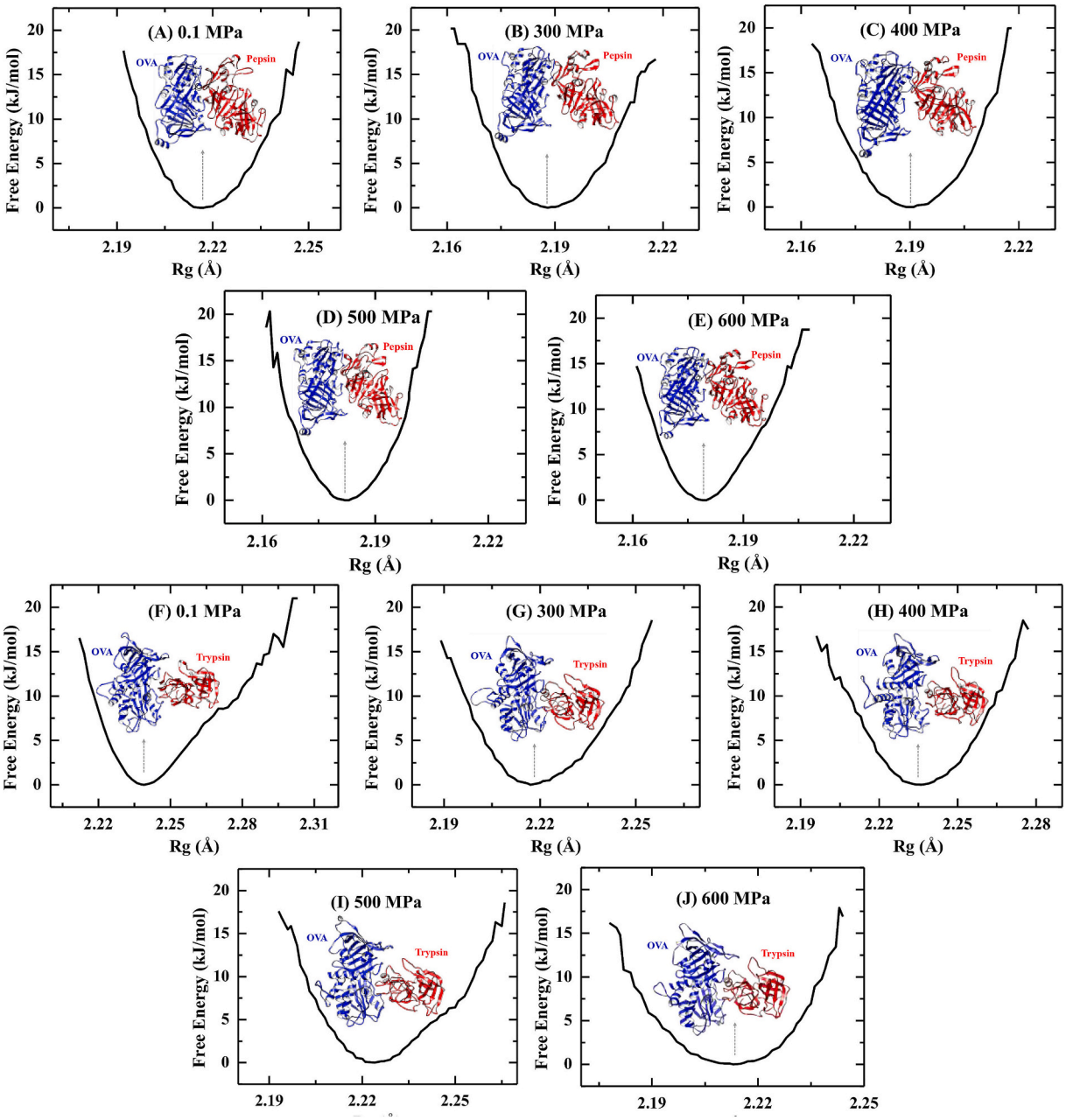

Fig. 4. Free energy (kJ/mol) as a function of the radius of gyration (Rg) for the OVA-pepsin (A-E) and OVA-trypsin (F-J) complexes across different pressures. The plot illustrates the structural compactness and stability of each complex by tracking changes in Rg and corresponding free energy at pressures of 0.1 MPa, 300 MPa, 400 MPa, 500 MPa and 600 MPa. Local minima structures are shown, representing energetically favorable conformations.

variations in the buried area across pressures. Similarly, the OVA-trypsin complex shows pressure-dependent interaction dynamics. At 0.1 MPa, the total surface area is 27,397.8 Å^2, with a ΔGint of −3.8 kcal/mol. At 300 MPa, the surface area decreases to 26,766.0 Å^2, and ΔGint becomes less favorable at −1.5 kcal/mol. At 400 MPa, the surface area is 26,838.9 Å^2, with a ΔGint of −1.4 kcal/mol. At 600 MPa, the surface area slightly increases to 27,108.3 Å^2, and ΔGint improves to −4.0 kcal/mol. The buried area reaches its maximum of 1920.6 Å^2 at 300 MPa, reflecting structural adjustments under varying pressures.

These findings demonstrate that both enzyme complexes exhibit pressure-dependent interaction dynamics, with stronger interactions observed at higher pressures. Notably, the OVA-trypsin complex displayed greater variability in binding strength with increasing pressure compared to the more consistent trend observed in the OVA-pepsin complex. The results confirm that epitope residues play a critical role in enzyme interactions, which are enhanced under high-pressure conditions. For instance, in the OVA-pepsin complex, ΔGint improved significantly from −0.9 kcal/mol at 0.1 MPa to −6.1 kcal/mol at 600 MPa. This enhanced interaction likely contributes to the reduced allergenicity of OVA under high-pressure treatment.

4. Discussion

The study of methods for desensitizing egg white protein is currently a hot topic of research both domestically and internationally. Non-thermal processing technologies are better at preserving the inherent nutritional components, color, and freshness of food. Among these, HHP has been used in the food industry as an alternative to heat treatment since it can improve the nutritional and functional properties, bioactivity, and modify the protein structure of food without affecting its

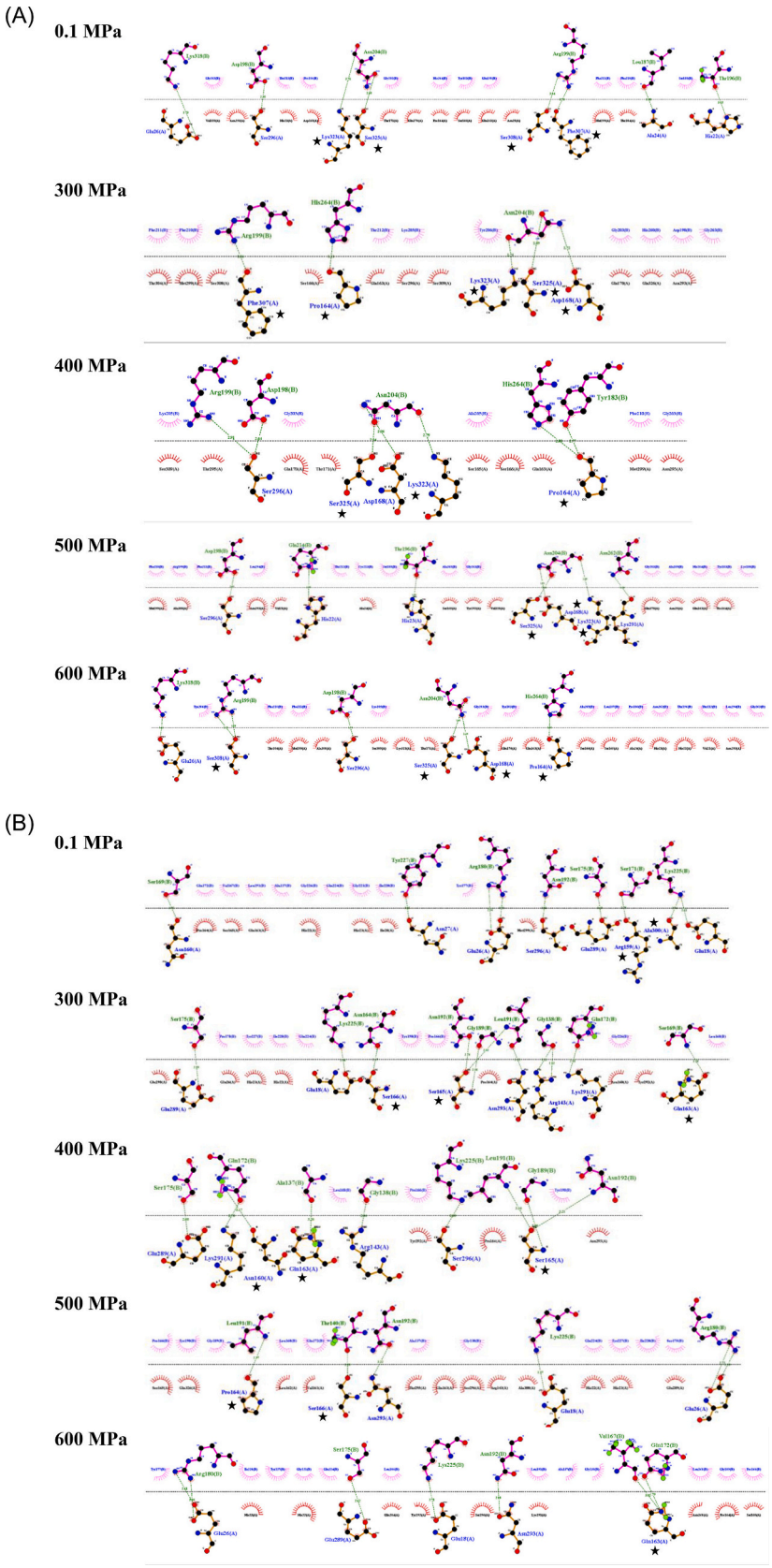

Fig. 5. Interaction diagram of the OVA-pepsin complex and OVA-trypsin complex. (A) Key hydrogen bonds and hydrophobic interactions between OVA (chain A) and pepsin (chain B) residues. (B) Key hydrogen bonds and hydrophobic interactions between OVA (chain A) and trypsin (chain B) residues. The figure highlights the binding interface, and the specific residues involved in stabilizing the complexes. ★ Marked residues were identified as part of OVA epitopes.

Table 1
Summary of surface area, buried area, interaction energy (ΔGint), and dissociation energy (ΔGdiss) for OVA-pepsin and OVA-trypsin complexes at various pressures.

Pressure (MPa)	Surface Area ($Å^2$)	ΔGint (kcal/mol)	Buried Area ($Å^2$)	ΔGdiss (kcal/mol)
OVA-Pepsin				
0.1	30,764.5	−0.9	1996.9	−9.3
300	29,839.8	−1.5	1505.5	−9.4
400	30,620.5	−0.8	1263.9	−10.4
500	29,851.9	−4.2	2041.2	−7.7
600	30,126.4	−6.1	1872.2	−4.0
OVA-Trypsin				
0.1	27,397.8	−3.8	1546.5	−4.3
300	26,766.0	−1.5	1920.6	−7.3
400	26,838.9	−1.4	1644.9	−7.6
500	26,720.7	−5.6	1680.2	−2.9
600	27,108.3	−4.0	1723.7	−4.1

sensory characteristics (Hogan et al., 2005). Our recent study has found that HHP treatment alters the structure and allergenicity of OVA protein (Yang et al., 2024). However, there have been no reports on the structural and allergenicity changes of OVA after gastrointestinal digestion following HHP treatment.

HHP technology can disrupt intermolecular forces and alter protein structures, showing potential for reducing protein allergenicity of OVA and Ovomucoid (OVM), another egg white protein allergen (Horvitz et al., 2024; Kanda et al., 2007; Panozzo et al., 2014; Yang et al., 2024). Gastrointestinal digestion can further affect the spatial structure and physiochemical characters of HHP-treated proteins. Studies simulating the gastrointestinal digestion process of OVA found that the α-helix structure content of OVA significantly decreased after digestion (Martos et al., 2010). In this study, CD spectroscopy revealed a 21.94 % decrease in the α-helix structure content of OVA after gastrointestinal digestion. HHP treatment caused OVA to unfold, exposing additional cleavage sites and further disrupting its spatial structure. Fluorescence spectroscopy, which measures the exposure of aromatic tryptophan residues, demonstrated a significant decrease in intrinsic fluorescence intensity after digestion. This decrease was likely due to protein unfolding and fluorescence quenching caused by exposed tryptophan residues. In addition, the increase in free sulfhydryl content and surface hydrophobicity observed after digestion supports these findings, suggesting that digestive enzymes disrupted disulfide bonds, leading to protein unfolding. A reduction in zeta potential indicated fewer negatively charged residues on the protein surface, while increased hydrophobicity and free sulfhydryl content reflected the exposure of buried hydrophobic cores, disrupting intramolecular cross-links (Jin et al., 2021). HHP treatment further enhanced OVA hydrolysis during digestion, contributing to the observed structural and physicochemical changes. Similar trends have been reported for other proteins. For example, after *in vitro* digestion, chicken protein exhibited reduced fluorescence intensity, indicating tertiary structure disruption (Bai et al., 2023). HHP-treated rice bran protein (200 MPa) showed improved solubility, emulsifying activity, and stability, accompanied by increased free sulfhydryl content and changes in secondary and tertiary structures (Wang et al., 2021a). Additionally, conformational changes in shrimp myosin after physical processing exposed cleavage sites for pepsin and trypsin, improving digestibility and reducing allergenicity (Zhang, Zhang, Chen, & Zhou, 2018). Collectively, these findings highlight that physical processing, such as HHP treatment, combined with simulated gastrointestinal digestion, is effective in enhancing the hydrolysis of OVA and modifying its spatial structure, potentially reducing its allergenicity.

Digestive stability is one of the common characteristics of most food allergens. This study showed that after gastrointestinal digestion, the microstructure of OVA changed from smooth, regularly shaped flakes to irregular fragments with a rough surface and holes. The degree of hydrolysis of OVA significantly increased after gastrointestinal digestion and the SDS-PAGE results showed bands appearing near the low molecular weight region, indicating that gastrointestinal digestion altered the molecular weight of OVA. This study is consistent with the previous findings (Benede, Perez-Rodriguez, & Molina, 2022). It has been reported that after 120 min of gastrointestinal digestion of peanut protein, there is a reduction in high molecular weight proteins, an enrichment of peptides with molecular weights below 10 kDa, partial hydrolysis of Ara h 1 and Ara h 3, and a significant reduction in IgE binding capacity (Rao, Tian, Fu, & Xue, 2018). OVM is degraded into 4.5–6.0 kDa peptides after gastric digestion and the IgE binding capacity of these hydrolyzed peptides is significantly reduced (Takagi et al., 2005). The potential effectiveness of heat/pressure treatments to reduce allergenicity have been investigated from several gastrointestinal (GI) digestion studies. HHP treatments (600 and 800 MPa) induces the rapid digestion of β-Lg and the production of peptide products (less than 1500 Da), which resulted in the reduction of β-Lg (Zeece et al., 2008). The higher digestibility of the HHP-treated whey protein isolate (WPI) with pepsin has no impact on the IgE-binding of the proteolysis products, compared to native WPI, probably because of the release, in both cases, of specific IgE-binding peptides (Chicón et al., 2008). Roasting induces the unfolding of the structure in shrimp (*Penaeus vannamei*), and gastrointestinal digestion can destroy the epitopes exposed by roasting and reduce its allergenicity (Liu et al., 2023). The residual immunoreactivity of the GI-resistant peptides in heat/pressure-treated (134 °C and 2 atm) almond protein from *in vitro* digestion showed that epitopes associated with known allergens were destroyed (De Angelis et al., 2018). However, other *in vitro* digestion experiments on thermal/pressure processed (134 °C and 2 atm) peanuts confirmed the persistent immunoreactivity attributed to an allergen (Ara h 3) (Bavaro et al., 2018). In our study, 600 MPa may enhance the interaction of OVA with pepsin/trypsin, resulting in the breakdown more epitopes, and preventing recognition by IgE receptors. However, the allergenicity of residues after gastrointestinal digestion may vary due to different digestive stability among processed food allergens.

This study highlights the significant impact of HHP on the structural stability and interactions of OVA with digestive enzymes, shedding light on its potential to reduce allergenicity. The protein-protein docking and MD simulations provide detailed insights into the interaction dynamics under various pressure conditions. The Rg is an important metric as it reflects the overall compactness of the protein, while free energy (ΔGint) provides a measure of the stability of the systems. Understanding these parameters is crucial for elucidating how external pressure influences the structural and conformational stability of protein in a complex environment. At 600 MPa, the lower Rg and ΔGint indicated that high-pressure environments favor more stable enzyme-substrate complexes. Additionally, regions spanning Met299 to Gln326 and Val328 to Pro386, which interact with both enzymes, were previously identified as epitopes (Behzad Gazme et al., 2022; Yang et al., 2024). Residues involved in hydrogen bond interactions such as Pro164, Asp168, Phe307, Ser308, Lys323, and Ser325 of OVA with pepsin, and Asn160, Gln163, Pro164, Ser165, and Ser166 of OVA with trypsin have been previously identified as epitope residues in experimental investigations and our previous study (Behzad Gazme et al., 2022; Yang et al., 2024). The identification of epitope residues in regions affected by HHP treatment supports the hypothesis that enzyme binding can mitigate allergenic properties. Significant changes in the β-sheet structure were observed at the pepsin/trypsin binding site, particularly in the regions Met286-Glu290, Gln326-Ile335, and Met173-Gly183. These findings suggest that the involvement of epitope residues in enzyme interactions may affect IgE-binding epitopes within the protein, potentially reducing the allergenicity of OVA. Our findings align with previous studies showing that pepsin and trypsin disrupt allergenic epitopes (Foster, Kimber, & Dearman, 2013; Hu et al., 2021), thereby potentially reducing the ability of OVA to trigger immune responses. Importantly, while the docking and MD simulations provide valuable static and

dynamic information on these interactions, further *in vivo* studies are needed to validate whether the pressure-induced reduction in allergenicity translates into reduced IgE binding in real-life scenarios. Additionally, exploring the long-term effects of such treatments on protein functionality and digestibility could broaden the application of HHP in food processing for hypoallergenic product development.

5. Conclusion

This study explored the structural and allergenicity changes of HHP-treated OVA *in vitro* digestion. HHP (600 MPa) accelerated OVA enzymatic hydrolysis, altered its microstructure, and unfolded its molecular structure, enhancing interactions with pepsin/trypsin and breaking down more epitopes. The interaction dynamics of enzyme complexes were pressure-dependent, with stronger interactions observed at higher pressures. These findings confirm that epitope residues play a role in enzyme interactions and demonstrate that HHP treatment is associated with the modification of OVA's digestive stability and epitopes, providing a promising strategy for allergen reduction.

CRediT authorship contribution statement

Jing Yang: Writing – review & editing, Writing – original draft, Supervision, Project administration, Methodology, Funding acquisition, Conceptualization. **Nandan Kumar:** Writing – original draft, Methodology, Investigation, Formal analysis, Data curation. **Hong Kuang:** Writing – original draft, Methodology, Investigation, Formal analysis, Data curation. **Jiajia Song:** Writing – review & editing. **Yonghui Li:** Writing – review & editing, Supervision.

Declaration of competing interest

The authors declare no competing financial interests that could have influenced the work presented in this paper.

Acknowledgements

This study was supported by Natural Science Foundation of Chongqing (Grant No. CSTB2024NSCQ-MSX0745, cstc2021jcyj-msxmX0712).

Appendix A. Supplementary data

Supplementary data to this article can be found online at https://doi.org/10.1016/j.foodchem.2025.142962.

Data availability

The data that has been used is confidential.

References

Abraham, M. J., Murtola, T., Schulz, R., Páll, S., Smith, J. C., Hess, B., & Lindahl, E. (2015). GROMACS: High performance molecular simulations through multi-level parallelism from laptops to supercomputers. *SoftwareX, 1*, 19–25.

Bai, X., Shi, S., Kong, B., Chen, Q., Liu, Q., Li, Z., Wu, K., & Xia, X. (2023). Analysis of the influencing mechanism of the freeze–thawing cycles on in vitro chicken meat digestion based on protein structural changes. *Food Chemistry, 399*, Article 134020.

Bavaro, S. L., Di Stasio, L., Mamone, G., De Angelis, E., Nocerino, R., Canani, R. B., … Monaci, L. (2018). Effect of thermal/pressure processing and simulated human digestion on the immunoreactivity of extractable peanut allergens. *Food Research International, 109*, 126–137.

Benede, S., Perez-Rodriguez, L., & Molina, E. (2022). Caco-2 cell response induced by peptides released after digestion of heat-treated egg white proteins. *Foods, 11*(22).

Bjelkmar, P., Larsson, P., Cuendet, M. A., Hess, B., & Lindahl, E. (2010). Implementation of the CHARMM force field in GROMACS: Analysis of protein stability effects from correction maps, virtual interaction sites, and water models. *Journal of Chemical Theory and Computation, 6*(2), 459–466.

Boukil, A., Marciniak, A., Mezdour, S., Pouliot, Y., & Doyen, A. (2022). Effect of high hydrostatic pressure intensity on structural modifications in mealworm (*Tenebrio molitor*) proteins. *Foods, 11*(7), 956.

Brodkorb, A., Egger, L., Alminger, M., Alvito, P., Assunção, R., Ballance, S., Bohn, T., Bourlieu-Lacanal, C., Boutrou, R., & Carrière, F. (2019). INFOGEST static *in vitro* simulation of gastrointestinal food digestion. *Nature Protocols, 14*(4), 991–1014.

Bu, G., Luo, Y., Chen, F., Liu, K., & Zhu, T. (2013). Milk processing as a tool to reduce cow's milk allergenicity: A mini-review. *Dairy Science & Technology, 93*(3), 211–223.

Chicón, R., Belloque, J., Alonso, E., & López-Fandiño, R. (2008). Immunoreactivity and digestibility of high-pressure-treated whey proteins. *International Dairy Journal, 18*(4), 367–376.

De Angelis, E., Bavaro, S. L., Forte, G., Pilolli, R., & Monaci, L. (2018). Heat and pressure treatments on almond protein stability and change in immunoreactivity after simulated human digestion. *Nutrients, 10*(11), 1679.

Foster, E. S., Kimber, I., & Dearman, R. J. (2013). Relationship between protein digestibility and allergenicity: Comparisons of pepsin and cathepsin. *Toxicology, 309*, 30–38.

Gazme, B., Rezaei, K., & Udenigwe, C. C. (2020). Effect of enzyme immobilization and in vitro digestion on the immune-reactivity and sequence of IgE epitopes in egg white proteins. *Food & Function, 11*(7), 6632–6642.

Gazme, B., Rezaei, K., & Udenigwe, C. C. (2022). Epitope mapping and the effects of various factors on the immunoreactivity of main allergens in egg white. *Food & Function, 13*(1), 38–51.

Hogan, E., Kelly, A. L., & Sun, D.-W. (2005). High pressure processing of foods:An overview. *Emerging Technologies for Food Processing*, 3–24.

Horvitz, S., Arroqui, C., & Vírseda, P. (2024). Mild high hydrostatic pressure processing: Effects on techno-functional properties and allergenicity of ovalbumin. *Journal of Food Engineering, 364*, Article 111797.

Hu, J., Yuan, L., An, G., Zhang, J., Zhao, X., Liu, Y., Shan, J., & Wang, Z. (2021). Antigenic activity and epitope analysis of β-conglycinin hydrolyzed by pepsin. *Journal of the Science of Food and Agriculture, 101*(4), 1396–1402.

Jiang, S., Xia, D., Zhang, D., Chen, G., & Liu, Y. (2020). Analysis of protein profiles and peptides during *in vitro* gastrointestinal digestion of four Chinese dry-cured hams. *LWT, 120*, Article 108881.

Jin, J., Okagu, O. D., Yagoub, A. E. A., & Udenigwe, C. C. (2021). Effects of sonication on the *in vitro* digestibility and structural properties of buckwheat protein isolates. *Ultrasonics Sonochemistry, 70*, Article 105348.

Kanda, Y., Hara, T., Matuno, M., Suzuki, A., Jho, T., & Odani, S. (2007). Effects of combined high-pressure/enzymatic treatment on the antigenicity of Ovomucoid. *High Pressure Bioscience and Biotechnology, 1*(1), 259–263.

Krissinel, E., & Henrick, K. (2007). Inference of macromolecular assemblies from crystalline state. *Journal of Molecular Biology, 372*(3), 774–797.

Kumar Sarma, H., & Sastry, G. N. (2022). Repurposing of approved drug molecules for viral infectious diseases: A molecular modelling approach. *Journal of Biomolecular Structure and Dynamics, 40*(17), 8056–8072.

Kumar, & Sastry, G. N. (2021). Study of lipid heterogeneity on bilayer membranes using molecular dynamics simulations. *Journal of Molecular Graphics and Modelling, 108*, Article 108000.

Kumar, Y. B., Kumar, N., John, L., Mahanta, H. J., Vaikundamani, S., Nagamani, S., … Sastry, G. N. (2024). Analyzing the cation-aromatic interactions in proteins: Cation-aromatic database V2. 0. *Proteins: Structure, Function, and Bioinformatics, 92*(2), 179–191.

Kumar, Y. B., Kumar, N., Vaikundamani, S., Nagamani, S., Mahanta, H. J., Sastry, G. M., & Sastry, G. N. (2023). Analyzing the aromatic-aromatic interactions in proteins: A2ID 2.0. *International Journal of Biological Macromolecules, 253*, Article 127207.

Li, Y., Zhang, S., Ding, J., Zhong, L., Sun, N., & Lin, S. (2022). Evaluation of the structure-activity relationship between allergenicity and spatial conformation of ovalbumin treated by pulsed electric field. *Food Chemistry, 388*(15), Article 133018.

Liu, K., Lin, S., Gao, X., Wang, S., Liu, Y., Liu, Q., & Sun, N. (2023). Reduced allergenicity of shrimp (Penaeus vannamei) by altering the protein fold, digestion susceptibility, and allergen epitopes. *Journal of Agricultural and Food Chemistry, 71*(23), 9120–9134.

Martos, G., Contreras, P., Molina, E., & Lopez-Fandino, R. (2010). Egg white ovalbumin digestion mimicking physiological conditions. *Journal of Agricultural and Food Chemistry, 58*(9), 5640–5648.

Nielsen, P., Petersen, D., & Dambmann, C. (2001). Improved method for determining food protein degree of hydrolysis. *Journal of Food Science, 66*(5), 642–646.

Panozzo, A., Manzocco, L., Calligaris, S., Bartolomeoli, I., Maifreni, M., Lippe, G., & Nicoli, M. C. (2014). Effect of high pressure homogenisation on microbial inactivation, protein structure and functionality of egg white. *Food Research International, 62*, 718–725.

Pekar, J., Ret, D., & Untersmayr, E. (2018). Stability of allergens. *Molecular Immunology, 100*, 14–20.

Rao, H., Tian, Y., Fu, W., & Xue, W. (2018). In vitro digestibility and immunoreactivity of thermally processed peanut. *Food and Agricultural Immunology, 29*(1), 989–1001.

Takagi, K., Teshima, R., Okunuki, H., Itoh, S., Kawasaki, N., Kawanishi, T., Hayakawa, T., Kohno, Y., Urisu, A., & Sawada, J. (2005). Kinetic analysis of pepsin digestion of chicken egg white ovomucoid and allergenic potential of pepsin fragments. *International Archives of Allergy and Immunology, 136*(1), 23–32.

Taniguchi, H., Ogura, K., Sato, S., Ebisawa, M., & Yanagida, N. (2022). Natural history of allergy to hen's egg: A prospective study in children aged 6 to 12 years. *International Archives of Allergy and Immunology, 183*(1), 14–24.

Varadi, M., Anyango, S., Deshpande, M., Nair, S., Natassia, C., Yordanova, G., Yuan, D., Stroe, O., Wood, G., & Laydon, A. (2022). AlphaFold protein structure database: Massively expanding the structural coverage of protein-sequence space with high-accuracy models. *Nucleic Acids Research, 50*(1), 439–444.

Wang, J., Wang, J., Vanga, S. K., & Raghavan, V. (2021). Influence of high-intensity ultrasound on the IgE binding capacity of act d 2 allergen, secondary structure, and in-vitro digestibility of kiwifruit proteins. *Ultrasonics Sonochemistry, 71*, Article 105409.

Wang, X., Tu, Z., Ye, Y., Liu, G., Wang, H., & Hu, Y. (2021). Mechanism on the allergenicity changes of α-lactalbumin treated by sonication-assisted glycation during in vitro gastroduodenal digestion. *Journal of Agricultural and Food Chemistry, 69*(24), 6850–6859.

Wang, S., Wang, T., Sun, Y., Cui, Y., Yu, G., & Jiang, L. (2021a). Effects of high hydrostatic pressure pretreatment on the functional and structural properties of rice bran protein hydrolysates. *Foods, 11*(1).

Wang, X., Tu, Z., Ye, Y., Liu, G., Hu, Y., & Wang, H. (2022). Isolation and allergenicity evaluation of glycated α-lactalbumin digestive products and identification of allergenic peptides. *Food Chemistry, 390*(1), Article 133185.

Yan, Y., & Huang, S. (2020). Modeling protein–protein or protein–DNA/RNA complexes using the HDOCK webserver. *Protein Structure Prediction*, 217–229.

Yang, J., Kuang, H., Kumar, N., Song, J., & Li, Y. (2024). Changes of structure properties and potential allergenicity of ovalbumin under high hydrostatic pressures. *Food Research International, 190*, Article 114658.

Zeece, M., Huppertz, T., & Kelly, A. (2008). Effect of high-pressure treatment on in-vitro digestibility of β-lactoglobulin. *Innovative Food Science & Emerging Technologies, 9*(1), 62–69.

Zhang, Y., Wang, W., Zhou, R., Yang, J., Sheng, W., Guo, J., & Wang, S. (2018). Effects of heating, autoclaving and ultra-high pressure on the solubility, immunoreactivity and structure of major allergens in egg. *Food and Agricultural Immunology, 29*(1), 412–423.

Zhang, Z., Zhang, X., Chen, W., & Zhou, P. (2018). Conformation stability, in vitro digestibility and allergenicity of tropomyosin from shrimp (Exopalaemon modestus) as affected by high intensity ultrasound. *Food Chemistry, 245*, 997–1009.

Zhu, Y., Vanga, S. K., Wang, J., & Raghavan, V. (2018). Impact of food processing on the structural and allergenic properties of egg white. *Trends in Food Science & Technology, 78*, 188–196.